

Qiang GAO, Dunbao YAN, Yunqi FU, Naichang YUAN

Loaded-frequency selective surface

© Higher Education Press and Springer-Verlag 2008

Abstract A new frequency-selective surface (FSS) with loadings is introduced in this paper and analyzed by way of period moment methods (PMMs). The simulated results show that FSS may operate in different bands and especially generate a large reduction in the resonant frequency for a fixed unit cell size through different loadings. This provides a new orientation in the development for FSS. Practical circuits are fabricated, and the measured results agree well with the simulated results.

Keywords loaded frequency selective surface (LFSS), lumped element, distributed element, period moment methods (PMMs)

1 Introduction

Frequency-selective surfaces (FSSs) have widespread application over much of the electromagnetic spectra. The frequency responses of the FSS highly depend on the configurations and spacing of the elements as well as on the thickness and permittivity of the dielectric layers that may be part of the screens. Figure 1 shows the equivalent circuit models [1–3] of the FSS, which the lumped inductances and capacitances can substitute for the periodic cell. Because the frequency responses may be altered by changing the inductances and capacitances, various FSSs can be realized by loading the distributed and lumped parameters.

2 Analysis

The cells of the three FSSs are presented in Fig. 2. The field scattered from the periodical structure of the FSS

can be formulated by utilizing the periodic moment method (PMM) [4–6]. The pertinent equation to be solved in this paper is:

$$E_t^{\text{inc}}(\mathbf{r}) + E_t^{\text{scat}}(\mathbf{r}) = \begin{cases} 0; & \text{distributed parameters} \\ Z_s \mathbf{J}; & \text{lumped parameters} \end{cases}, \quad (1)$$

where $Z_s = Z_L \Delta W / \Delta L$ is equivalent surface impedance of lumped parameters, while Z_L is loaded in the region of $\Delta W \times \Delta L$.

In the MoM procedure, the subdomain bases of the rooftop functions and Galerkin technique are employed to solve the unknown induced currents.

3 Simulation and experimental results

The three proposed resonant cells in Fig. 2 are realized on the substrate, $\epsilon_r = 3.0$ and $h = 0.5$ mm. All the cells are closed and packed on square lattices and the period P is 16 mm. Figures 3 (a), (b) and (c) show the transmission coefficients of Figs. 2 (a) and (b) at normal incidence and that of TE 45° and TM 45° respectively. It is evident that the higher resonance shifts toward the low frequency (7.7–6.8 GHz), while the lower resonance remains stable for Fig. 2 (b). This is because the higher resonance is caused by the interior loop and the loaded circular patch, which brings self-inductances and extra distributed capacitances between the interior loop and the patch, giving more impact on the interior loop than the exterior one. Figure 3 (d) presents the transmission coefficients of Fig. 2 (b) in different radii at normal incidence. The larger the radius is, the lower the higher resonance will be.

Figure 4 (a) shows the transmission coefficients of Figs. 2 (c) and (a) at normal incidence. Because the lumped capacitances are loaded between the exterior loops and the lower resonance basically depended on the exterior loop, the lower resonance switches intensely and the higher one shifts slightly. Figure 4 (b) shows the transmission coefficients of Fig. 2 (c) with different capacitances at normal incidence. The larger the capacitances are, the lower the lower resonance will be.

Translated from *Chinese Journal of Radio Science*, 2006, 21(3): 441–444 [译自: 电波科学学报]

Qiang GAO (✉), Dunbao YAN, Yunqi FU, Naichang YUAN
Microwave Center, School of Electronic Science and Engineering,
National University of Defense Technology, Changsha 410073,
China
E-mail: gq19790324@163.com

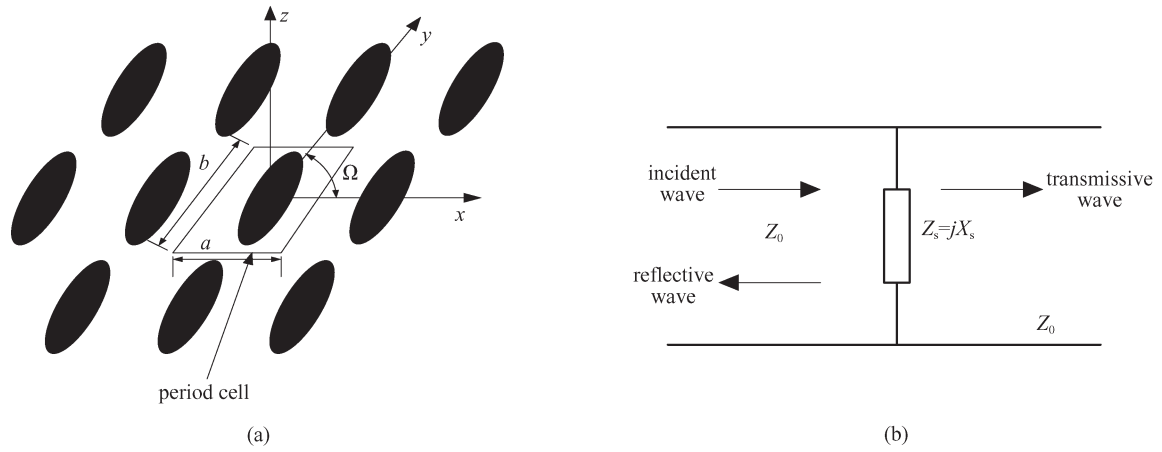


Fig. 1 (a) Free-standing FSS; (b) equivalent circuit models (X_s is the combination of the lumped L and C)

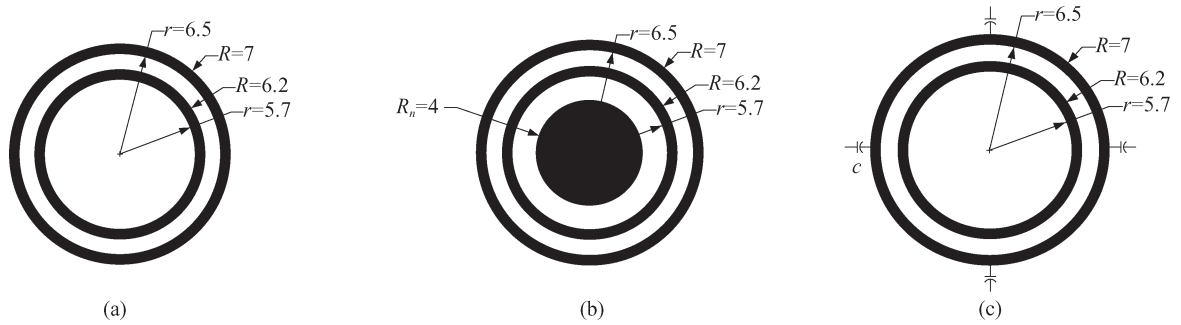


Fig. 2 Shapes of resonant cells /mm

(a) Double loop; (b) double loop loaded in the circular patch; (c) double loop loaded in the lumped capacitances

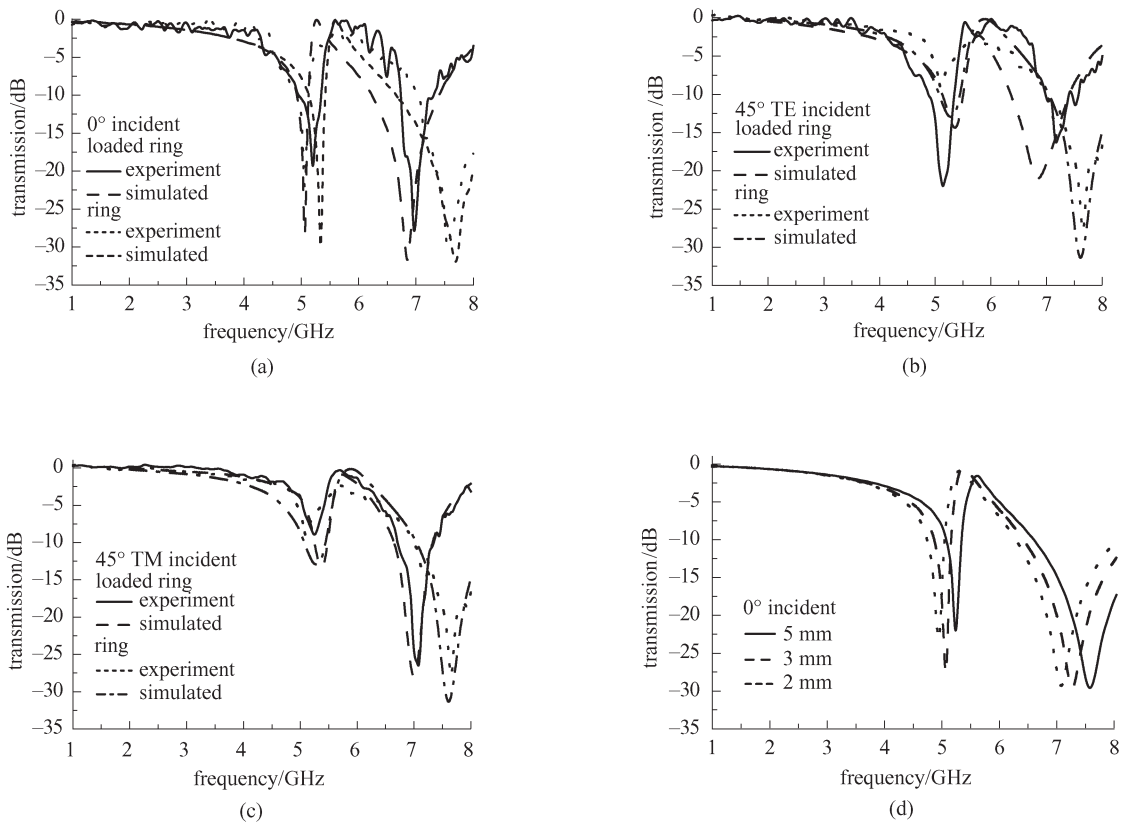


Fig. 3 Transmission coefficients of Figs. 2 (a) and (b)

(a) Normal incidence; (b) 45° TE incidence; (c) 45° TM incidence; (d) normal incidence of the circular patches in different radii

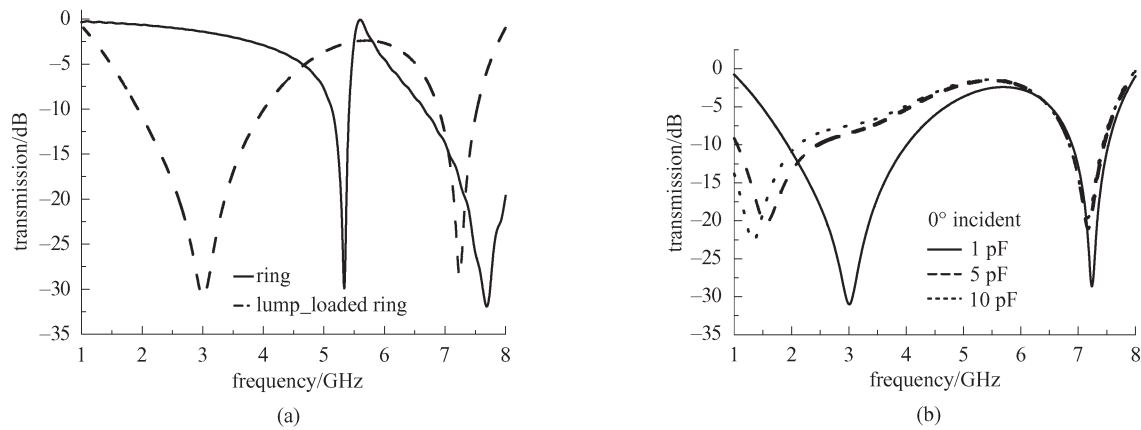


Fig. 4 Transmission coefficients at normal incidence

(a) Transmission coefficients of Figs. 2(a) and (c); (b) transmission coefficients of different loaded lumped capacitances

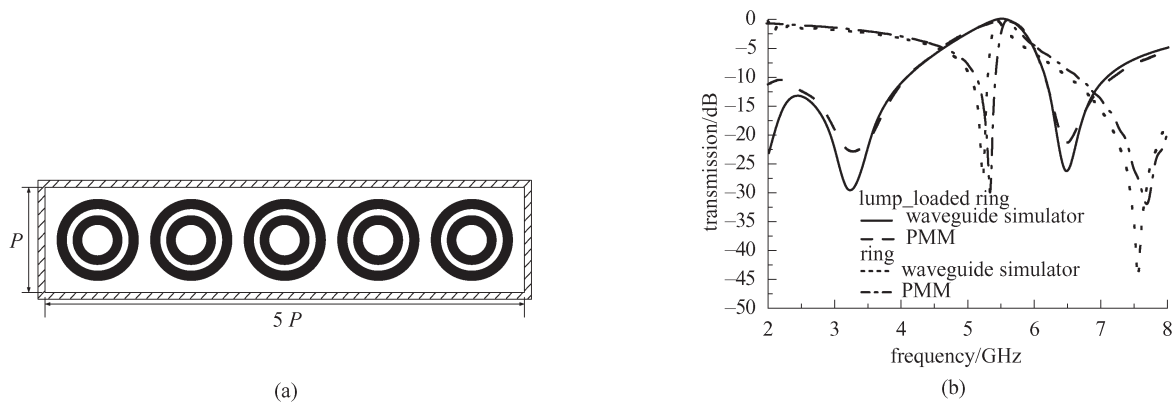


Fig. 5 Waveguide simulator. (a) Cross section; (b) results of WGS and PMM

Waveguide simulators (WGS) [7,8] feature as a convenient means of verifying infinite array calculations. The frequency and the scanning angle in a waveguide operating in the TE_{10} mode are related by

$$\sin\theta = \frac{\lambda_0}{\lambda_c}, \quad (2)$$

where λ_c is the cutoff wavelength of the guide. Figure 5 shows the waveguide simulator and the results of PMM and WGS. They are basically in agreement.

4 Conclusions

This paper has described a new type of frequency-selective surface based on the distributed and lumped loadings. This FSS can change the resonances through different loadings and realize the operations in different bands. A waveguide simulator was presented and demonstrated to confirm the theory adopted for analysis.

Acknowledgements This work was supported by the Major Fundamental Preliminary Research Foundation for National Security (No. 51307).

References

1. Ben A. Munk. Frequency Selective Surface Theory and Design. New York: Wiley, 2001
2. Mias C. Frequency selective absorption using lumped element frequency selective surfaces. *Electronics Letters*, 2003, 39(11): 847–849
3. Tennant A, Chambers B. A single-layer tunable microwave absorber using an active FSS. *IEEE Microwave and Wireless Components Letters*, 2004, 14(1): 46–47
4. Mittra R, Chan C H, Cwik T. Techniques for analyzing frequency selective surfaces—a review. In: *Proceedings of the IEEE*, 1988, 76(12): 1593–1614
5. Chen C C. Transmission through a conducting screen perforated periodically with apertures. *IEEE Transactions on Microwave Theory and Techniques*, 1979, 18(9): 627–632
6. Rubin B J, Bertoni H L. Reflection from periodically perforated plane using a subsectional current approximation. *IEEE Transactions on Antennas and Propagation*, 1983, 31(6): 829–836
7. Amitay N, Galindo Y, Wu C P. Theory and analysis of phased array antennas. Wiley-Interscience, 1972
8. Wheeler H A. A survey of the simulator techniques for designing a radiation element in a phased-array antenna. In: *Proceedings of Symposium on Phased Array Antennas*, 1970, 157–172